Journal of Thermal Analysis and Calorimetry, Vol. 95 (2009) 3, 871–876

PHYSICO-CHEMICAL CHARACTERIZATION OF ANHYDROUS *D*-MANNITOL

G. Bruni[1*], *V. Berbenni*[1], *C. Milanese*[1], *A. Girella*[1], *P. Cofrancesco*[1], *G. Bellazzi*[2] *and A. Marini*[1]

[1]C.S.G.I. – Dipartimento di Chimica Fisica 'M. Rolla', Università degli Studi di Pavia, Viale Taramelli 16, 27100 Pavia, Italy
[2]GlaxoSmithKline, via Fleming 2, 37135 Verona, Italy

In this work the solid-state characterization of anhydrous *D*-mannitol has been performed: α and β modifications can be distinguished only by XRPD and FTIR as they show melting temperature and enthalpy that are the same within the standard deviation. The understanding of the thermal behaviour of the δ form (obtained by re-crystallization in acetone) has required XRPD experiments performed at variable temperature. This form during heating undergoes a solid phase transition to α modification. By cooling a melted sample, under a wide range of experimental conditions, a very fast crystallization occurs. Independently of the starting crystal form (β or δ form), the re-crystallization of *D*-mannitol from melt always leads to α form.

Keywords: *DSC, D-mannitol, polymorphism, thermal analysis, X-ray powder diffraction*

Introduction

D-mannitol (Fig. 1) is a hexa-hydric alcohol and one of the most common excipients in pharmaceutical lyophilized products due to its tendency to crystallize from properly cooled aqueous solutions and to the relatively high melting point of the eutectic mixture mannitol/ice [1, 2]. These features end in obtaining a stable and good-looking solid as it is required for a pharmaceutical product. Actually some problems are still unresolved such as the generation of pressure inside the reaction vial that causes its breakage during the freeze-drying process [3, 4] and consequently considerable economic losses for industries. Over the years several authors [5–9] individuated a number of polymorphs and differently named some of them that, later on, proved to be the same. This fact obviously has generated a confusing picture. In this work a physico-chemical characterization of *D*-mannitol has been carried out with the aim to gain further knowledge on its behaviour and on the interconversion of its different polymorphs.

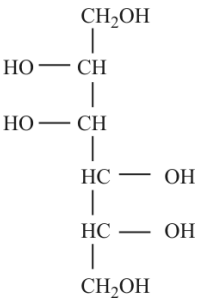

Fig. 1 Structural formula of *D*-mannitol

Experimental

Material

D-mannitol came from a single batch of industrial production (Roquette, batch n° E1253/1348).

The measurements were performed on commercial sample both as received and after it underwent melting. Also a re-crystallized sample was examined. The re-crystallized sample was prepared by adding acetone to a hot saturated aqueous solution of *D*-mannitol. The obtained crystals were rapidly filtered and washed with acetone. The solid was stored in a desiccator.

Apparatus and procedures

Scanning electron microscopy (SEM)

Sample micrographs were collected with a scanning electron microscope Cambridge Stereoscan 200 (UK) on gold sputtered samples.

X-ray powder diffraction (XRPD)

X-ray powder diffraction (CuK_α radiation) data were collected with a Bruker D5005 (Bruker Siemens, Germany) system equipped with a θ–θ vertical goniometer and a Position Sensitive Detector (PSD, Braun). Patterns were recorded in step scan mode (step: 0.015°, counting time: 0.5 s) in the angular range 2ϑ=5–30°. A polythermal chamber was used to collect data under dry nitrogen atmosphere at controlled temperature.

* Author for correspondence: bruni@matsci.unipv.it

1388–6150/$20.00

Akadémiai Kiadó, Budapest, Hungary
Springer, Dordrecht, The Netherlands

Differential scanning calorimetry (DSC)

DSC measurements were performed with a TA Q2000 calorimeter interfaced with a TA 5000 data system (TA Instruments Inc., New Castle, DE) and equipped with a refrigerated cooling system (RCS90) suitable for subambient temperature measurements down to –90°C. Measurements were performed at different heating rates in the temperature range 25–200°C on samples (4–5 mg) placed in standard open or closed pans of aluminum under dry nitrogen flow (45 mL min^{-1}). Temperature and enthalpy calibrations were performed by running indium samples (purity: 99.999%).

Moreover samples were subjected to cyclic thermal treatments directly into DSC cell with the following thermal protocol: i) first heating up to 180°C; ii) cooling; iii) second heating to 200°C. Cooling was performed with different protocols:

- Cooling at different rates (in the range 0.3–60 K min^{-1}) down to 25 or –60°C.
- Cooling at 1 K min^{-1} down to 117°C with an isothermal step (90 min) at this temperature followed by controlled (1 K min^{-1}) cooling to room temperature.
- Quenching of the sample by removing the DSC pan and putting it into liquid nitrogen.

All data from thermal measurements are averages of three or more experiments.

Thermogravimetric analysis (TGA)

Thermogravimetric analysis was performed with a TA 2950 thermobalance interfaced with a TA Q5000 data system (TA Instruments Inc., New Castle, DE). Samples (about 5 mg) were scanned from room temperature to 180°C at 10°C min^{-1} in dry nitrogen (45 mL min^{-1}).

FTIR spectroscopy

FTIR spectra by diffuse reflectance were performed with a Nicolet FTIR 730 Spectrometer equipped with a DRIFT collector by Spectra Tech – UK. Samples (3% by mass in anhydrous KBr) were thoroughly mixed and the spectra were collected by co-adding 512 scans in the 4000–400 cm^{-1} range at 2 cm^{-1} resolution.

Results and discussion

Commercial and melted re-crystallized D-mannitol

DSC experiments were performed with a thermal protocol basically constituted by a heating–cooling–heating cycle as described in the experimental section.

As concerns the first heating ramp, the DSC trace of commercial sample (2 K min^{-1}, closed pan, Fig. 2a) only shows a sharp endothermic peak due to melting. The onset temperature and the relevant enthalpy change are respectively: T_{onset}=165.83±0.14°C; ΔH=280.07±3.99 J g^{-1}. The melting parameters during heating do not depend on pan configuration (open and closed) nor on heating rate. The thermogravimetric analysis does not show any appreciable mass change in the temperature range of interest (25–180°C) suggesting that the sample is thermally stable over melting.

By cooling procedure 1 (cooling at different rates down to 25 or –60°C), a very sharp exothermic peak shows up (Fig. 2b), due to crystallization, with a considerable extent of super-cooling and with a heat release that causes a spike in the time-temperature straight-line (Fig. 2b). In the case of cooling procedure 2 (cooling at 1 K min^{-1} down to 117°C with isothermal step at this temperature followed by controlled cooling at 1 K min^{-1} to room temperature), the temperature of 117°C was selected as it is slightly higher than that

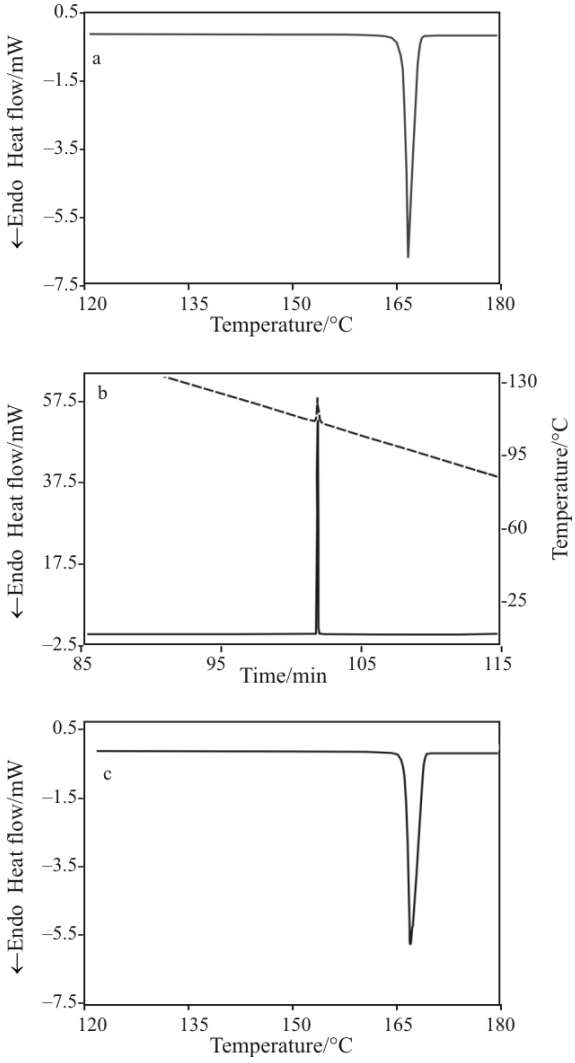

Fig. 2 DSC curves of commercial *D*-mannitol recorded at 2 K min^{-1} in closed pan: a – first heating, b – cooling, c – second heating

where the mentioned sudden crystallization takes place with cooling procedure 1 (at the same cooling rate). Surprisingly, a very sharp exothermic peak now sets up during the isothermal stage, after about 70 min at 117°C. Also in this case such a peak is associated with a spike in the time-temperature straight-line.

Second heating (2 K min^{-1}, Fig. 2c) was performed on the samples cooled according to procedures 1, 2 and 3. Since different cooling protocols have been chosen, we would expect that different solid forms would have crystallized and then melted. However, we found that the values of the melting parameters are very clustered independent of the cooling procedure (they are also independent of pan configuration and heating rate).

The onset temperature and the enthalpy change of the endothermic peak obtained from a large number of measurements are respectively: T_{onset}=165.59±0.07°C; ΔH=277.49±4.41 J g^{-1}. This suggests that the solid phase obtained by the different cooling procedures is the same (melted re-crystallized solid). The mean values of melting parameters in the second heating are slightly lower than the values found in the first heating. However the values of the two series fit well together within the relevant standard deviations so that it is impossible to maintain, on the basis of thermal measurements, that the commercial sample is different from the melted re-crystallized one.

On the contrary XRPD patterns (Figs 3a and b) indicate that the two samples are different solid forms. In particular the XRPD pattern (Fig. 3a) of the

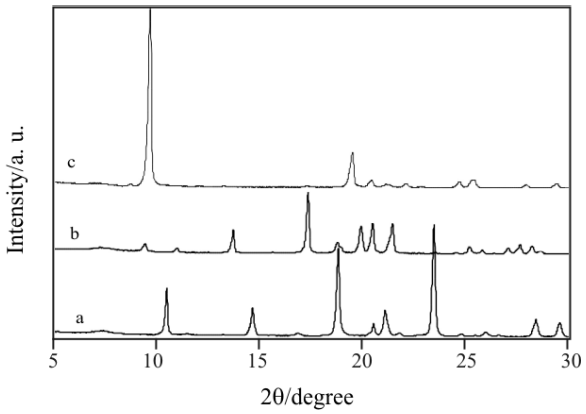

Fig. 3 XRPD patterns at room temperature of a – commercial, b – melted re-crystallized, c – acetone re-crystallized *D*-mannitol

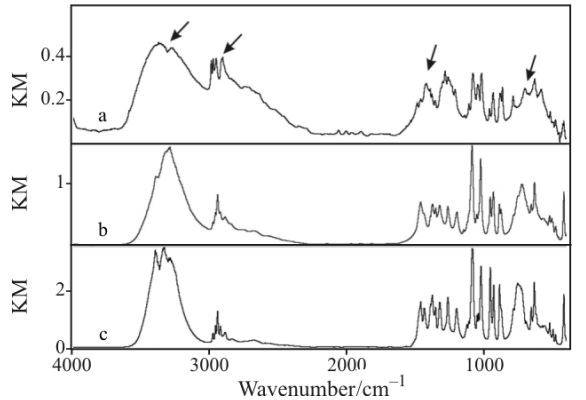

Fig. 4 FTIR spectra of a – commercial, b – melted re-crystallized, c – acetone re-crystallized *D*-mannitol

Table 1 Wavenumbers (cm^{-1}) of the IR spectra of the different solid forms of *D*-mannitol

Remarks	Wavenumbers		
	commercial sample	melted re-crystallized sample	acetone re-crystallized sample
OH stretching	3366 (very broad)	3282 (broad)	3391–3324 (broad)
CH stretching	2983–2947–2901	2937+shoulders	2952–2938–2916
CH_2 scissor	1417	1458	1458 (1431)
	no peak	1371	1373 (1351)
1350–1260 1 and 2° alcohol OH plane deformation	1280 1260	1320 1261	1320 1261
Skeletal vibration	no peak	1194	1196
1085–1030 (s) 1° alcohol CO stretching 1125–1085 (s) 2° alcohol CO stretching	1080 1042 1015	1086 1021	1083 1019
Fingerprint region	957 930 881–864 785 (sharp)–698 628 416	952 928 884 724 (very board) 630 416	952 926 884 751 (very broad) 631 416

commercial sample corresponds to that of the β form (JCPDS n° 22–1797) while the pattern of the melted re-crystallized sample (Fig. 3b) corresponds to that of the α form (JCPDS n° 22–1793).

The FTIR spectra (Figs 4a and b) also confirm that the commercial and melted re-crystallized sample are constituted by different solid forms (Table 1). By observing Fig. 4 it can be observed that the spectra of the two samples show differences in all the mid-IR wavenumber range. So the diffuse band due to the –OH stretching is broader in the commercial than in the melted sample. Furthermore this band is centred at two different frequencies (3366 cm^{-1} in the commercial *D*-mannitol and 3282 cm^{-1} in the melted *D*-mannitol). Moreover the stretching of the $–CH_2–$ and of –CH– residues shows a very different aspect too. Again pronounced differences are present as regards the bands due to –OH deformation. This is true either for the in plane –OH deformation (see the broad band centred at ≈1280 cm^{-1} in the commercial sample and the quite narrow peak at 1261 cm^{-1} in the melted one) and for the out of plane deformation (see the broad band centred at ≈750 cm^{-1} in the commercial sample and the multiple band centred at ≈630 cm^{-1} with relative maxima at 785, 698 and 578 cm^{-1} in the case of the melted sample).

Furthermore, the morphology of the commercial and melted re-crystallized samples is also different. The commercial sample is formed by sticks of about 200 μm size; small particles stuck on the surface of the larger ones (Fig. 5a). The melted re-crystallized sample, on the contrary, shows irregular particles and the growth of crystals along a preferential direction can be noted (Fig. 5b).

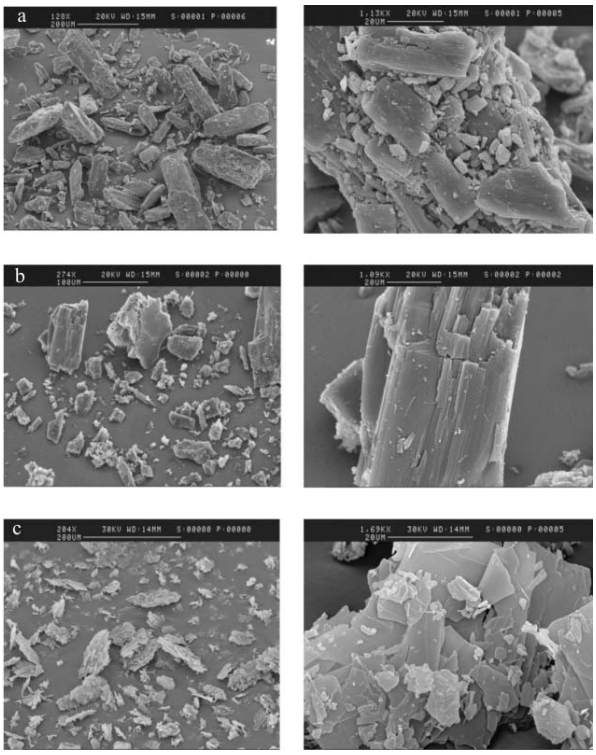

Fig. 5 SEM photographs at two different magnifications of a – commercial, b – melted re-crystallized, c – acetone re-crystallized *D*-mannitol

Acetone re-crystallized samples

By thermogravimetric analysis it was possible to assess that no solvent is present in this sample.

The DSC traces recorded in the thermal cycle are shown in Fig. 6. The thermal behaviour of the crystallized sample is different, over first heating, from that of the commercial one: indeed the melting peak (Fig. 6a) is preceded by a weak endo-exothermal effect (inset of Fig. 6a). While the melting onset temperature (T_{onset}=165.64±0.04°C) is the same, within the experimental error, as those recorded on the commer-

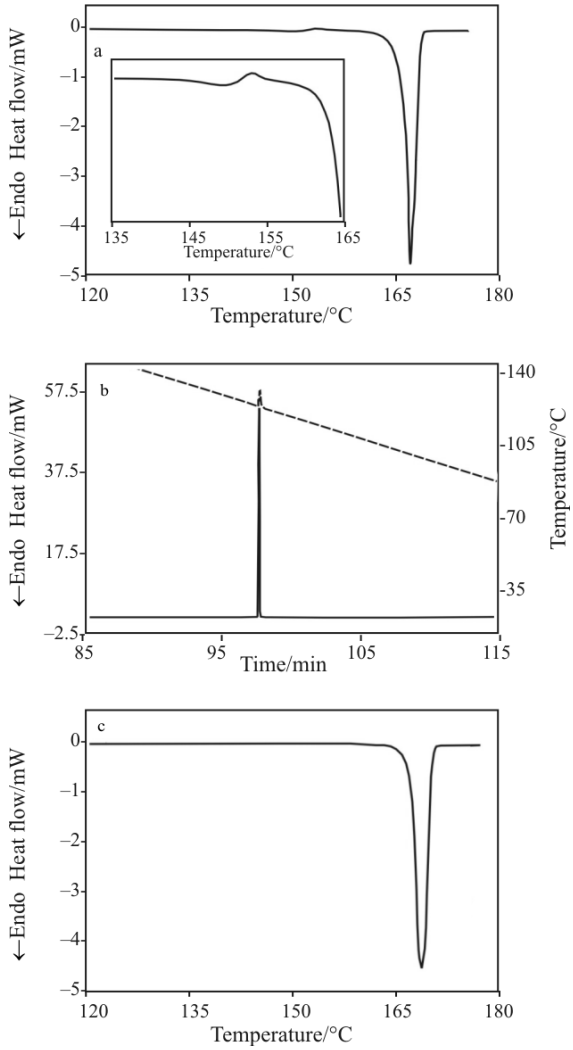

Fig. 6 DSC curve recorded at 2 K min^{-1} in closed pan of acetone re-crystallized *D*-mannitol: a – first heating, b – cooling, c – second heating

cial and melted re-crystallized samples, the melting enthalpy (ΔH=267.17±2.51 J g^{-1}) is slightly lower [commercial sample (β form): ΔH=280.07±3.99 J g^{-1}; melted re-crystallized sample (α form): ΔH=277.49±4.41 J g^{-1}]. The thermal behaviour of the acetone re-crystallized sample during cooling is very similar to that shown by the commercial sample (Fig. 6b). Finally the melting parameters during second heating (Fig. 6c, T_{onset}=165.37±0.08°C; ΔH=269.00±2.78 J g^{-1}) are undistinguishable from those obtained over the first heating as it is the case with the commercial sample. Figure 5c shows the morphology of the sample re-crystallized from acetone: it can be seen that it is constituted by aggregates of very thin platelets.

The XRPD patterns (Fig. 3c) and the IR spectrum (Fig. 4c) of the acetone re-crystallized sample are different from those of the β and the α forms and agree well with the ones reported in literature for the δ form (JCPDS n° 22-1794). The IR spectrum of the acetone re-crystallized sample shows differences compared to that of the melted sample both in the high frequency region and in the fingerprint zone. In the high frequency region the band due to the stretching of the –OH groups is centred at ≈3283 cm^{-1}, in the case of the melted sample, while it is centred at ≈3324 cm^{-1} in the case of the acetone re-crystallized sample. The difference in the fingerprint region is mainly due to the broad band due to the –OH out of plane deformation that is centred at ≈750 cm^{-1} in the case of the melted sample while it is centred at a lower frequency (≈724 cm^{-1}) in the case of the acetone re-crystallized sample. On the other hand the XRPD pattern and FTIR spectrum show that the solid obtained by cooling the melted δ form is constituted by α form as it is the case with the melted re-crystallized β form. Thus the re-crystallization of *D*-mannitol from melt always leads to α form independently of the starting crystal form (β or δ form).

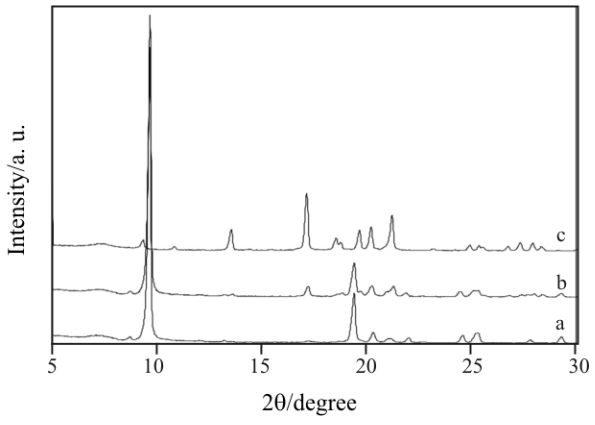

Fig. 7 XRPD patterns of acetone re-crystallized *D*-mannitol at different temperatures: a – room temperature, b – 135, c – 148°C

In order to understand the processes responsible for the endo-exothermal effect recorded during the first heating in the temperature range 135–160°C (inset in Fig. 6a), XRPD patterns at variable temperatures were recorded on the acetone re-crystallized sample and are shown in Fig. 7. The pattern remains substantially unchanged up to 125°C; at 135°C (Fig. 7b), temperature that corresponds to the onset of the endothermic peak, some diffraction peaks characteristic of the α modification appear (2ϑ≈13.7, 17.2, 19.8, 21.3, 28.5°). At 148°C (Fig. 7c), temperature that lies near the maximum of the endothermic peak, the pattern has become that of the α form. This evidence allows to account for the endothermic peak, that corresponds to the δ→α transition. It is impossible to give a reliable value of the transition enthalpy due to the overlapping of this peak with the exothermic one. However we may infer that it is low, meaning that the δ→α transition implies only minor changes; this is confirmed by the very tiny differences between the vibrational spectra of the two forms (Table 1).

The X-ray pattern of the sample remains unchanged at least up to 153°C, meaning that the sample is still in solid form after the endo-exothermal peak occurred and that such a solid form is the same present just before the exothermic peak. Thus our data do not agree with those reported by Burger *et al*. [8] who attribute the endothermic peak to melting of the δ form and the exothermic one to solidification of the melt to give β and/or α modifications. We think that the exothermic peak could be attributed to the crystallization toward α modification of a little amount of amorphous phase present in the acetone re-crystallized sample. Based upon the interpretation proposed of the endo-exothermic peak, it is the α form that undergoes melting rather

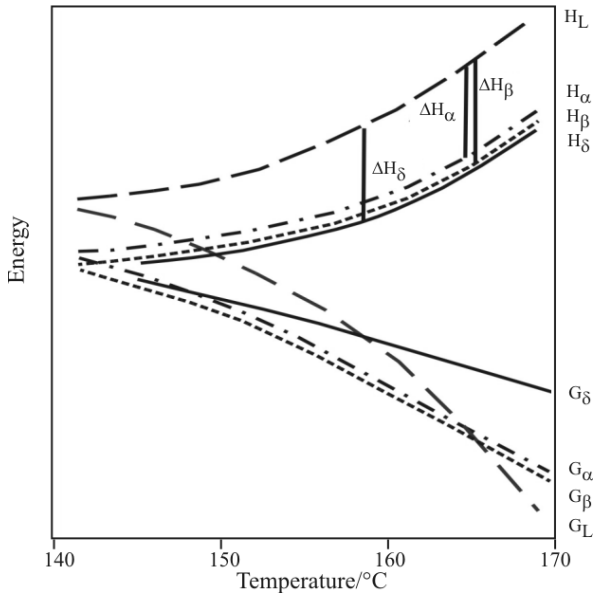

Fig. 8 Energy-temperature diagram of *D*-mannitol polymorphs

than the δ form. However, the melting enthalpy of the sample is slightly lower than that expected for the α form. Such a difference could be attributed to an incomplete crystallization of the amorphous phase at the origin of the exothermic peak. This hypothesis is confirmed by DSC measurements with an isothermal step at 140°C for 6 h. In the subsequent heating the endo-exothermic effect is missing and the melting enthalpy increases to a value (ΔH=274.35±3.04 J g^{-1}) very similar to that recorded on the α form obtained by melting and cooling down to room temperature the commercial sample.

The results so far obtained make it possible to propose the energy–temperature diagram of the three polymorphs (Fig. 8). According to the heat of fusion rule [10], a monotropic relationship exists between α and β modifications since the α form, the lowest melting crystal modification, is never thermodynamically stable. An enantiotropic relationship exists, on the contrary, between δ and α modifications. Both forms have their own stability temperature range. We never saw a transition between δ and β forms. Thus the relationship between these two forms is still far from certain.

Conclusions

In this work the characterization of the three polymorphs of *D*-mannitol has been carried out and the relationships between them have been defined. While the α and β modifications show different X-ray and IR spectra, they are undistinguishable by thermal analysis. Between these polymorphs exists a monotropic relationship: the α form is never thermodynamically stable. The thermal behaviour of the δ form has been explained thanks to high temperature diffraction measurements. During heating, the δ form changes to α modification before undergoing melting. The thermal behaviour of the melted samples, i.e. the very fast crystallization and release of high amount of heat, are the most interesting points that could be at the origin of the breakage of vials during freeze-drying.

Acknowledgements

We are grateful to GlaxoSmithKline (Verona, Italy) for providing *D*-mannitol powder.

References

1 N. A. Williams, Y. Lee, G. P. Polli and T. A. Jennings, J. Parent. Sci. Technol., 40 (1986) 135.
2 E. Yonemochi, Y. Yoshioka, Y. Yoshihashi and K. Terada, J. Therm. Anal. Cal., 85 (2006) 693.
3 N. A. Williams and T. Dean, J. Parent. Sci. Technol., 45 (1991) 94.
4 N. A. Williams and J. Guglielmo, J. Parent. Sci. Technol., 47 (1993) 119.
5 H. S. Kim, G. A. Jeffrey and R. D. Rosenstein, Acta Cryst., B24 (1968) 1449.
6 H. M. Berman, G. A. Jeffrey and R. D. Rosenstein, Acta Cryst., B24 (1968) 442.
7 F. R. Fronczek, H. N. Kamel and M. Slattery, Acta Cryst. Section - Crystal Struct. Commun., C59 (2003) 567.
8 A. Burger, J. Henck, S. Hetz, J. M. Rollinger, A. A. Weissnicht and H. Stöttner, J. Pharm. Sci., 89 (2000) 457.
9 C. E. Botez, P. W. Stephens, C. Nunes and R. Suryanarayanan, Powder Diffr., 18 (2003) 214.
10 A. Burger and R. Ramberger, Mikrochim. Acta II, 2 (1979) 273.

Received: June 22, 2008
Accepted: October 14, 2008
OnlineFirst: January 13, 2009

DOI: 10.1007/s10973-008-9384-5